PHYSICAL REVIEW A **90**, 041603(R) (2014)

Atom-dimer scattering and stability of Bose and Fermi mixtures

Xiaoling Cui
Beijing National Laboratory for Condensed Matter Physics, Institute of Physics, Chinese Academy of Sciences, Beijing, 100190, People's Republic of China

(Received 9 June 2014; published 21 October 2014)

Motivated by a recent experiment by the Ecole Normale Supérieure de Lyon (ENS) group on the mixture of Bose and Fermi superfluids [I. Ferrier-Barbut *et al.*, Science **345**, 1035 (2014)], we investigate the effective scattering between a bosonic atom and a molecule (dimer) of fermion atoms. It is found that the mean-field prediction of the atom-dimer scattering length ($a_{\rm ad}$), as simply given by the boson-fermion scattering length ($a_{\rm bf}$), generically fails. Instead, $a_{\rm ad}$ crucially depends on the ratio between $a_{\rm bf}$ and $a_{\rm ff}$ (the fermion-fermion scattering length), and in addition it log-periodically depends on the three-body parameter. We identify the universal parameters in characterizing $a_{\rm ad}$ for a wide range of $a_{\rm ff}$ in the molecular side of the fermion-fermion Feshbach resonance, and further demonstrate that the atom-dimer many-body system can become unstable against either phase separation or collapse as tuning $a_{\rm ff}$. Our results have some implications for the ENS experiment.

DOI: 10.1103/PhysRevA.90.041603 PACS number(s): 67.85.Pq, 05.30.−d, 34.50.−s

The dilute ultracold atomic gases with highly tunable interactions provide an ideal platform for studying the fundamental yet challenging few-body problems, among which the Efimov physics undoubtedly takes a prominent place due to its intriguing properties [1,2]. In the 1970s, Efimov established two important laws, the scaling law and the radial law, for the bound states of three identical bosons interacting with a single s-wave scattering length a_s [1]. The scaling law predicts the discrete scaling symmetry, i.e., a change of a_s by a scaling factor $\chi = e^{\pi/s_0}$ (where $s_0 = 1.00624$) corresponds to the energy changed by a factor χ^{-2}. The radial law predicts that at $a_s > 0$ side, the atom-dimer scattering length $a_{\rm ad}$ can be parametrized by a_s and a three-body parameter measuring the short-range interactions among the three particles, and $a_{\rm ad}$ diverges periodically as varying a_s by a scaling factor χ. These predictions have been successfully verified in cold-atom experiments on various homo- and heteronuclear systems, by observing the enhanced three-body recombination at $a_s < 0$ [3–11], the atom-dimer loss resonance at $a_s > 0$ [12–15], the Efimov spectrum measured from radio-frequency spectroscopy [16,17], and recently the successive three-body loss peaks directly confirming the discrete scaling symmetry [18–20].

Recently, the Ecole Normale Supérieure de Lyon (ENS) group has reported a new breakthrough in realizing a mixture of Bose-Einstein condensation and fermionic superfluidity using lithium isotopes [21]. In this experiment, the fermion-fermion scattering length ($a_{\rm ff}$) can be tuned over several orders of magnitude via a Feshbach resonance, while the boson-fermion scattering length ($a_{\rm bf}$) almost stays static. This brings new challenges to the few-body physics as mainly in the following two aspects. First, in the presence of more than one scattering length, the original Efimov predictions for single a_s could be greatly affected. Second, given the realized extremely low temperature, the few-body physics will no doubt fundamentally influence the low-energy collective phenomena in a dilute many-body system, which have been rarely discussed before in this setup. Also considering a variety of multicomponent systems [4–6,13–15] that can be potentially cooled down to a quantum degenerate regime, it is thus imperative to investigate the few-body physics in these systems and their general consequences in a many-body environment.

With the above motivations, in this work we study the effective scattering between a bosonic atom and a dimer of two fermions, with tunable $a_{\rm ff}$ and nonvarying $a_{\rm bf}$. By establishing a generalized Efimov radial law, we show that the atom-dimer scattering length $a_{\rm ad}$ sensitively depends on the ratio between the two scattering lengths, $x = a_{\rm bf}/a_{\rm ff}$, and can even go across resonance as tuning x. In addition, it log-periodically depends on the three-body parameter κ^*, similar to that of identical bosons. Its general formula is

$$\frac{a_{\rm ad}}{a_{\rm bf}} = C_1(x) + C_2(x)\cot[s_0\ln(\kappa^*|a_{\rm bf}|) + \Phi(x)]. \quad (1)$$

Here C_1, C_2, Φ are all universal functions in terms of x. We numerically verify this formula and extract those universal functions for a wide range of x (taking equal mass of boson and fermion, for instance). Moreover, we show that the mean-field prediction of $a_{\rm ad}$, which is proportional to $a_{\rm bf}$ as determined from the boson-fermion density-density interaction, generically fails for typical cold-atom systems with short-range interactions. Furthermore, based on Eq. (1), we show that the stability of the atom-dimer many-body system can be greatly altered by tuning x, where the homogenous mixture can become unstable against phase separation or collapse. We identify the according phase diagram for several typical values of $a_{\rm bf}$ and κ^*. Finally we point out some implications of our results for the ENS experiment [21].

Model. Considering two distinguishable fermions at positions $\mathbf{r}_1$, $\mathbf{r}_2$ with mass m_f and one boson at $\mathbf{r}_3$ with mass m_b, the Hamiltonian can be written as $\hat{H} = \hat{H}_0 + \hat{U}$,

$$\hat{H}_0 = -\frac{\nabla_{\mathbf{r}}^2}{2\mu} - \frac{\nabla_{\boldsymbol{\rho}}^2}{2\mu_\rho};$$
$$\hat{U} = U_{\rm ff}\delta(\mathbf{r}) + U_{\rm bf}\left[\delta\left(\boldsymbol{\rho} + \frac{\mathbf{r}}{2}\right) + \delta\left(\boldsymbol{\rho} - \frac{\mathbf{r}}{2}\right)\right]. \quad (2)$$

Here $\mathbf{r} = \mathbf{r}_2 - \mathbf{r}_1$ and $\boldsymbol{\rho} = \mathbf{r}_3 - (\mathbf{r}_1 + \mathbf{r}_2)/2$, respectively, describe the relative motion between two fermions and between the boson and the center of mass of fermions; the correspond-

ing masses are $\mu = m_f/2$ and $\mu_\rho = 2m_f m_b/(2m_f + m_b)$. $U_{\rm bf}$ ($U_{\rm ff}$) is the bare interaction between boson-fermion (fermion-fermion) and can be related to $a_{\rm bf}$ ($a_{\rm ff}$) via $\frac{1}{U_{\rm bf}} = \frac{\bar\mu}{2\pi a_{\rm bf}} - \frac{1}{V}\sum_{\mathbf{k}} \frac{2\bar\mu}{k^2}$ ($\frac{1}{U_{\rm ff}} = \frac{\mu}{2\pi a_{\rm ff}} - \frac{1}{V}\sum_{\mathbf{k}} \frac{2\mu}{k^2}$), where $\bar\mu = m_b m_f/(m_b + m_f)$, and V is the volume.

Now we study the atom-dimer elastic scattering between the boson and the dimer of fermions. The associated energy is $E = -\epsilon_{\rm ff}$, where $\epsilon_{\rm ff} = 1/(2\mu a_{\rm ff}^2)$ is the dimer binding energy. We solve the wave function Ψ using the Lippmann-Schwinger equation $|\Psi\rangle = \hat G_0 \hat U |\Psi\rangle$, with $\hat G_0 = 1/(E - \hat H_0 + i\epsilon)$ the noninteracting Green's function. Introducing three auxiliary functions in

$$\langle \mathbf{r}, \boldsymbol{\rho}|\hat U|\Psi\rangle = f(\boldsymbol{\rho})\delta(\mathbf{r}) + g_+(\mathbf{r})\delta\left(\boldsymbol{\rho} + \frac{\mathbf{r}}{2}\right) + g_-(-\mathbf{r})\delta\left(\boldsymbol{\rho} - \frac{\mathbf{r}}{2}\right), \tag{3}$$

we arrive at three coupled equations in terms of f, g_+, and g_-, which correspond to implementing the boundary conditions to Ψ respectively at $\mathbf{r} \to 0$, $\boldsymbol{\rho} + \frac{\mathbf{r}}{2} \to 0$, and $\boldsymbol{\rho} - \frac{\mathbf{r}}{2} \to 0$ [22]. For instance, we have

$$\lim_{\mathbf{r}\to 0} \Psi(\mathbf{r}, \boldsymbol{\rho}) \sim f(\boldsymbol{\rho})(1/r - 1/a_{\rm ff}). \tag{4}$$

The physical meaning of the f function is thus transparent; it effectively describes the relative motion between the atom (boson) and the dimer (fermions) and can be referred to as an atom-dimer scattering wave function. The atom-dimer scattering length $a_{\rm ad}$ can be extracted from the Fourier transformation of the f function in $\mathbf{k}$ space,

$$f(\mathbf{k}) = (2\pi)^3\delta(\mathbf{k}) - \frac{4\pi a_{\rm ad}(\mathbf{k})}{k^2}, \tag{5}$$

with $a_{\rm ad} \equiv a_{\rm ad}(0)$ given by the on-shell atom-dimer T-matrix element at zero momentum.

Atom-dimer scattering with unequal scattering lengths has been studied before in a three-component Li6 system [23]. For our system, where the boson-fermion interactions are described by a single $a_{\rm bf}$, we have $g_+ = g_- \equiv g$ and finally we obtain two coupled integral equations for $a_{\rm ad}(\mathbf{k})$ and $g(\mathbf{k})$:

$$-\frac{4\pi a_{\rm ad}(\mathbf{k})}{k^2}\left(\frac{1}{U_{\rm ff}} - \frac{1}{V}\sum_{\mathbf{q}} \frac{1}{E - \frac{q^2}{2\mu} - \frac{k^2}{2\mu_\rho} + i\epsilon}\right) = \frac{1}{V}\sum_{\mathbf{p}} \frac{2g(\mathbf{p})}{E - \frac{(\mathbf{k}/2+\mathbf{p})^2}{2\mu} - \frac{k^2}{2\mu_\rho} + i\epsilon}; \tag{6}$$

$$g(\mathbf{p})\left(\frac{1}{U_{\rm bf}} - \frac{1}{V}\sum_{\mathbf{k}} \frac{1}{E - \frac{(\mathbf{k}/2+\mathbf{p})^2}{2\mu} - \frac{k^2}{2\mu_\rho} + i\epsilon}\right) = \frac{1}{E - \frac{p^2}{2\mu}} + \frac{1}{V}\sum_{\mathbf{k}}\left(\frac{-4\pi a_{\rm ad}(\mathbf{k})}{k^2\left(E - \frac{(\mathbf{k}/2+\mathbf{p})^2}{2\mu} - \frac{k^2}{2\mu_\rho} + i\epsilon\right)} + \frac{g(\mathbf{k})}{E - \frac{(\mathbf{p}-\mathbf{k})^2}{8\mu} - \frac{(\mathbf{p}+\mathbf{k})^2}{2\mu_\rho} + i\epsilon}\right). \tag{7}$$

Equations (6) and (7) generally apply to arbitrary mass ratios $\eta = m_f/m_b$ and arbitrary $x = a_{\rm bf}/a_{\rm ff}$. In this work we consider $m_b = m_f = m$ ($\eta = 1$), for instance, and mainly focus on the region $x \in (1, +\infty)\bigcup(-\infty, 0)$, where the fermion-fermion dimer is the ground-state dimer in the three-body system [24].

Generalized Efimov radial law. Before proceeding with numerical solutions from Eqs. (6) and (7), we first prove that $a_{\rm ad}$ can be parametrized explicitly by a few parameters and follows the universal form as in Eq. (1). This is a straightforward generalization of the Efimov radial law [1] to the case of multiple scattering lengths. For the proof, we only illustrate the main idea here, which contains two essential ingredients (here $R \sim \sqrt{\sum_{i<j} |\mathbf{r}_i - \mathbf{r}_j|^2}$ is the hyperradius; r_0 is the range of interaction potential):

(A) In the scale-invariant regime $r_0 \ll R \ll |a_{\rm bf}|, |a_{\rm ff}|$, the three-body potential is identical to that with three divergent scattering lengths and follows an attractive $1/R^2$ form. The resulting wave function is formulated as $\sin(s_0 \ln R + \theta)$, where θ is determined by the boundary condition at short-range $R \sim r_0$ and thus incorporates the three-body parameter κ^*. This formulation is unchanged in the presence of multiple scattering lengths.

(B) The atom-dimer elastic scattering is given by the asymptotic behavior of above three-body wave function at $R \gg |a_{\rm bf}|, |a_{\rm ff}|$. In order to identify that, one has to consider the intermediate regime of $R \sim |a_{\rm bf}|, |a_{\rm ff}|$. The interaction in this regime can be effectively considered as a certain potential barrier and thus is characterized by reflection and transmission coefficients, which are dimensionless numbers and can be parametrized by scattering lengths and the wave vector of the wave function. Given the barrier characteristics, one can formulate explicitly the evolution of the wave function from $R \ll |a_{\rm bf}|, |a_{\rm ff}|$ to $R \gg |a_{\rm bf}|, |a_{\rm ff}|$, and extract the atom-dimer phase shift or $a_{\rm ad}$ in the latter regime. The general form is as in Eq. (1). Compared to the original Efimov radial law [1], here the specialty is that we need multiple scattering lengths, $a_{\rm bf}$ and $a_{\rm ff}$, to characterize the barrier, and this leads to the dependence of those characterization coefficients (C_1, C_2, Φ) on the scattering length ratio x.

The universal formula of $a_{\rm ad}$ as in Eq. (1) can be numerically verified by exactly solving Eqs. (6) and (7) for different momentum cutoffs κ^*. In Fig. 1, we show $a_{\rm ad}/a_{\rm bf}$ as functions of $\kappa^* a_{\rm bf}$ for a typical value of $x(= 2)$, and the log-periodic fit to Eq. (1) is excellent (especially at large $\kappa^* a_{\rm bf}$). We have also computed for other positive and negative x and equally verified Eq. (1).

The validity of Eq. (1) in turn implies the breakdown of mean-field theory, which gives $a_{\rm ad} = 8/3 a_{\rm bf}$ by equating the density-density interaction between bosons and fermions with that between bosons and dimers [22]. In fact, this result corresponds to approximating $g(\mathbf{p})$ as $\frac{2\pi a_{\rm bf}/\bar\mu}{E - p^2/(2\mu)}$ in Eq. (7) and also enforcing $\kappa^* \gg 1/a_{\rm ff}$ in Eq. (6) [22]. Overall it requires $|a_{\rm bf}| \ll 1/\kappa^* \ll a_{\rm ff}$, where $1/\kappa^* \sim r_0$ is typically the range of interacting potential. Apparently under this requirement the system cannot be in the scale-invariant regime [which violates (A)] and one must take into account the finite-range effect. Given typical cold-atom systems with r_0 much shorter than the scattering lengths, we conclude that the mean-field prediction to $a_{\rm ad}$ generically fails.

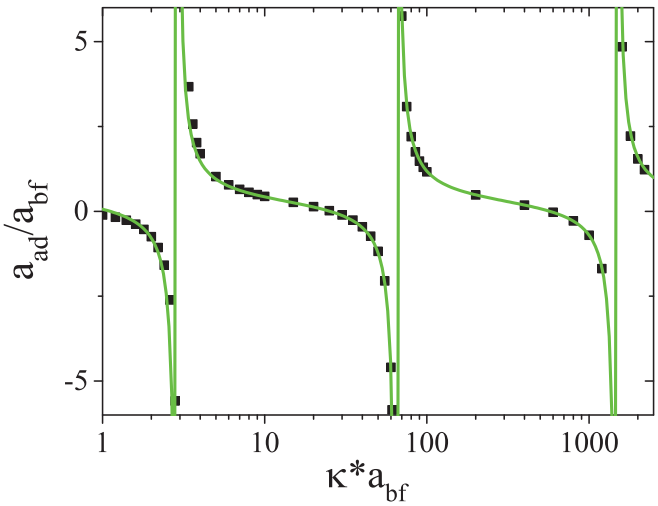

FIG. 1. (Color online) Verification of universal formula for a_{ad} [in units of a_{bf}, see Eq. (1)] at $x = a_{bf}/a_{ff} = 2$. The square points show numerical results by solving Eqs. (6) and (7) for different momentum cutoffs κ^*. The green curve is the fit to Eq. (1) with $s_0 = 1.00624$, $C_1 = 0.29$, $C_2 = 0.41$, $\Phi = -0.34\pi$. The fit gets more accurate for larger $\kappa^* a_{bf}$.

Universal functions. After establishing Eq. (1), one can numerically extract the three universal parameters C_1, C_2, Φ as functions of x. The results for both negative and positive x are shown in Fig. 2. Several conclusions can be drawn as follows.

First, Figs. 2(a1) and 2(a2) show that the amplitudes of both C_1 and C_2 decay at large $|x|$, which means that $|a_{ad}/a_{bf}|$ is generally very small (except near resonance) in the limit of $|a_{bf}| \gg a_{ff}$ ($|x| \gg 1$). This actually indicates a unitary regime when $a_{bf} \to \pm\infty$, where a_{ad} approaches a universal value that only depends on a_{ff} and κ^* but not a_{bf} any more. The existence of this regime is verified in Fig. 3(a), by plotting a_{ad} for fixed κ^* and a_{ff} while changing a_{bf} to $-\infty$ or $+\infty$. Exactly at

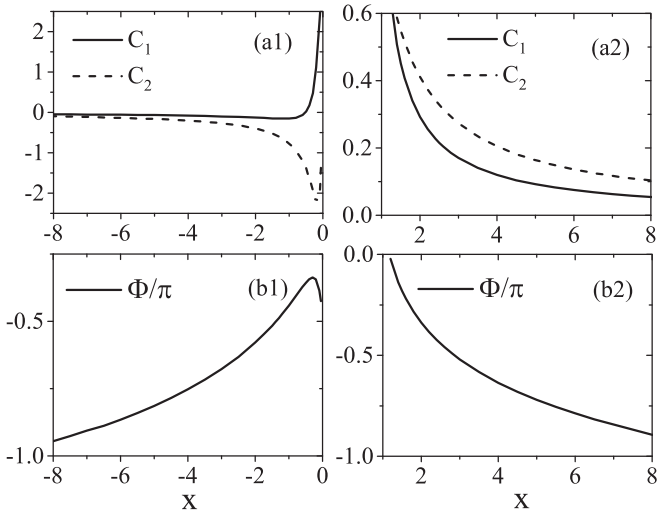

FIG. 2. Universal parameters C_1, C_2 (upper panel), and Φ (lower panel) as functions of x. In (a1) and (b1), $x < 0$; in (a2) and (b2), $x > 1$.

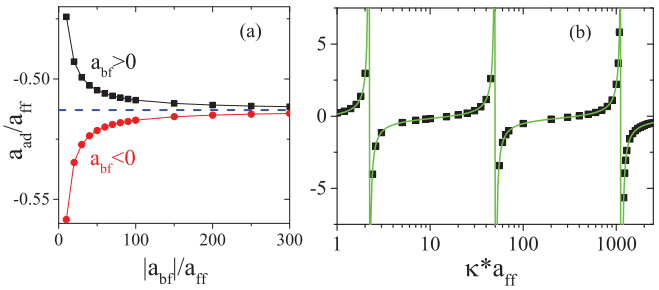

FIG. 3. (Color online) a_{ad} in the unitary limit of a_{bf}. The length unit here is a_{ff}. (a) a_{ad} as changing a_{bf} to $+\infty$ (black square) or $-\infty$ (red circle) for fixed $\kappa^* a_{ff} = 100$. The dashed horizontal line denotes the universal value $a_{ad}/a_{ff} = -0.513$ at unitarity ($|a_{bf}| = \infty$). (b) a_{ad} as a function of κ^* at $|a_{bf}| = \infty$. The green curve is the fit to Eq. (8).

$|a_{bf}| = \infty$, a_{ad} can be formulated as

$$\frac{a_{ad}}{a_{ff}} = c_1 + c_2 \cot[s_0 \ln(\kappa^* a_{ff}) + \phi], \quad (|a_{bf}| = \infty). \tag{8}$$

In Fig. 3(b), we show the log-periodic dependence of a_{ad}/a_{ff} on κ^*, and extract the three universal parameters as $(c_1, c_2, \phi) = (-0.15, -0.31, -0.25\pi)$. A similar formula as Eq. (8) was obtained previously in Li6 system with three scattering lengths [2].

Second, the dependence of the phase Φ on x, as shown in Figs. 2(b1) and 2(b2), implies that a_{ad} can also be tuned to resonance by changing x while fixing κ^*. Near the resonance position x_{res}, we have

$$\frac{a_{ad}}{a_{bf}} = \frac{W}{x - x_{res}} + \text{const}, \tag{9}$$

where $W = C_2(x_{res})/\Phi'(x_{res})$ is the resonance width. In Fig. 4(a), we show a typical resonance structure of a_{ad} as tuning x with a fixed κ^*. Accordingly, the width W is plotted in Fig. 4(b) for both positive and negative resonance position $x = x_{res}$. It is readily seen that the absolute value of W is of the order of 1 or even larger for most values of x, thus these resonances should be easy to resolve in cold-atom experiments given not so small a_{bf}. Such resonance structure of a_{ad} would significantly influence the stability of the atom-dimer many-body system, as demonstrated below.

Many-body phase diagram. For a many-body system composed of the boson condensate and the dimer (fermion-

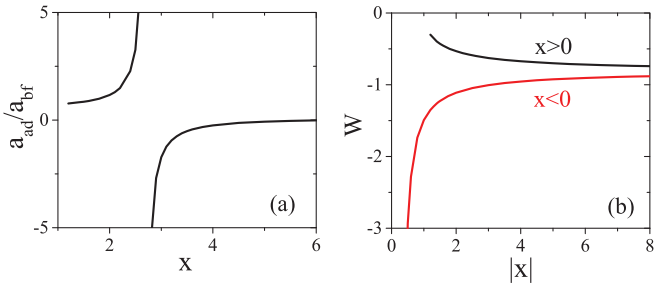

FIG. 4. (Color online) Resonance of a_{ad} by tuning x. (a) a_{ad}/a_{bf} as functions of x for fixed $\kappa^* a_{bf} = 100$. The resonance position is $x = 2.7$. (b) Resonance width W for positive (black line) and negative (red line) resonance position x.

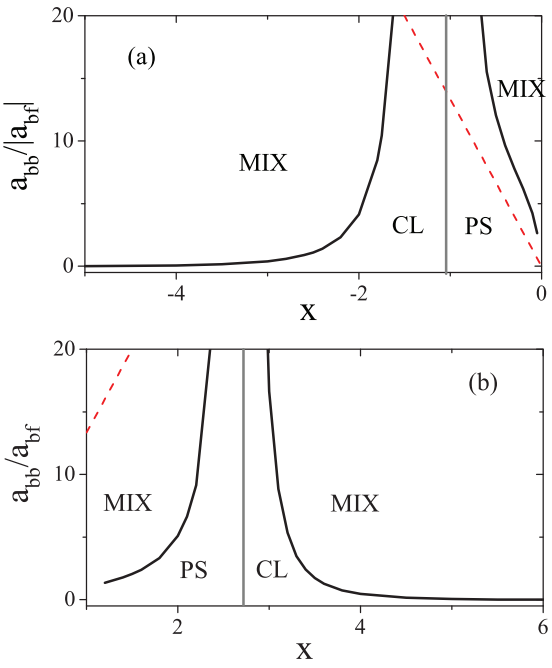

FIG. 5. (Color online) Many-body phase diagram of atom-dimer system for negative(a) and positive(b) $a_{\rm bf}$ and with a fixed $\kappa^*|a_{\rm bf}| = 100$. Three phases are shown: homogenous mixture (MIX), phase separation (PS), and collapse phase (CL). Black solid lines denote the phase boundaries between MIX and PS/CL. Gray vertical lines mark the atom-dimer resonances at $x = -1.21(a), 2.7(b)$, which also serve as PS-CL phase boundaries. Red dashed lines shows phase boundaries based on the mean-field prediction of $a_{\rm ad}$; above the boundary is MIX phase and below is CL (a) or PS (b) phase.

fermion) superfluid, the total energy density $\mathcal{E} = E/V$ can be written as [25]

$$\mathcal{E} = \frac{n_b^2}{2}\frac{4\pi a_{bb}}{m} + \frac{n_d^2}{2}\frac{2\pi a_{dd}}{m} + n_b n_d \frac{3\pi a_{\rm ad}}{m}, \qquad (10)$$

where n_b, n_d are respectively the density of bosons and dimers, and a_{bb}, $a_{dd}(= 0.6a_{\rm ff}$ [26]) are the boson-boson and dimer-dimer scattering lengths. The stability of a homogeneous mixture system can be examined through the second-order variation of the energy functional $\mathcal{E}$ with respect to the density fluctuations of the atoms and dimers [27]. Following the standard analysis, we arrive at three phases in different parameter regimes: (i) homogenous mixture (MIX) at $|a_{\rm ad}| < \xi$; (ii) phase separation (PS) at $a_{\rm ad} > \xi$; and (iii) collapse (CL) at $a_{\rm ad} < -\xi$, where $\xi = 0.73\sqrt{a_{bb}a_{\rm ff}}$. The system is unstable in (ii) and (iii) toward a spatial separation of atoms and dimers and the formation of a denser state containing both components [28]. The phase diagram can be deduced accordingly in the $(a_{bb}, a_{\rm ff})$ plane given that $a_{\rm ad}$ is known from few-body solutions [Eq. (1)].

In Fig. 5, we present the phase diagrams for both positive and negative $a_{\rm bf}$ with a fixed κ^*. Due to the resonance structure of $a_{\rm ad}$ as tuning x [as shown in Fig. 4(a)], the phase diagram is very rich. Typically, at a given a_{bb} and by increasing $|x|$, the system can go through four phases in the order MIX-PS-CL-MIX [29]. This is in distinct contrast to the phase diagram based on the mean-field prediction $a_{\rm ad} = 8/3a_{\rm bf}$, where only one phase boundary exists between MIX-PS or MIX-CL (see red dashed lines). Note that the reentrance of the MIX phase at large $|x|$ in Fig. 5 is due to the universal behavior of $a_{\rm ad}$ when $a_{\rm bf} \to \infty$, which scales as $a_{\rm ff}$ rather than keeps growing with $a_{\rm bf}$ as mean-field predicted. In this limit, the phase diagram can be straightforwardly obtained in the $(a_{bb}, a_{\rm ff})$ plane based on Eq. (8), which will not be shown here.

Implications for the ENS experiment [21]. Our results have some implications for the ENS experiment. We have shown that the mean-field evaluation of $a_{\rm ad}$ generically fails. Therefore at the deep molecular side of fermions, the dipole mode frequency shift of the bosons, $\delta\omega_b$, has to employ the exact solution of $a_{\rm ad}$ [our Eq. (1)] rather than Eq. (10) in Ref. [21]. Given the resonance structure of $a_{\rm ad}$ as tuning $a_{\rm ff}$ [our Fig. 4(a)], $\delta\omega_b$ is also expected to exhibit similar intriguing features in this regime. It is promising that by measuring the deviation of $\delta\omega_b$ from mean-field evaluations (based on the density-density interaction of bosons and fermions), one could see clearly how the mean-field theory breaks down as fermions gradually approach the molecule limit and the atom-dimer picture starts to develop.

Concluding remarks. In conclusion, we have established a general formula [Eq. (1)] for the atom-dimer elastic scattering in the Bose and Fermi mixture, and pointed out its significant effect on the stability of a many-body system. Remarkably, by tuning the ratio between the boson-fermion and fermion-fermion scattering lengths, we show that the atom-dimer scattering length $a_{\rm ad}$ can vary dramatically and even go across resonance. This invalidates the mean-field prediction of $a_{\rm ad}$, and suggests there should be more sophisticated treatment of the interaction energy as the system approaching the strong coupling limit of fermions. Moreover, our results show the possibility of tuning the effective interaction between a particle and a composite one simply by adjusting the internal interaction within the latter. This scheme can be generally applied to a vast class of ultracold boson and fermion mixtures [30] and is expected to significantly influence the many-body physics therein.

Acknowledgments. The author thanks Tin-Lun Ho for helpful discussions. This work is supported by National Nature Science Foundation of China (NSFC) under Grants No. 11104158 and No. 11374177, and programs of the Chinese Academy of Sciences.

[1] V. Efimov, Sov. J. Nucl. Phys. **12**, 589 (1971) [Yad. Fiz. **12**, 1080 (1970)]; Sov. J. Nucl. Phys. **29**, 546 (1979) [Yad. Fiz. **29**, 1058 (1979)].

[2] E. Braaten and H.-W. Hammer, Phys. Rep. **428**, 259 (2006).

[3] T. Kraemer, M. Mark, P. Waldburger, J. G. Danzl, C. Chin, B. Engeser, A. D. Lange, K. Pilch, A. Jaakkola, H.-C. Nägerl, and R. Grimm, Nature **440**, 315 (2006).

[4] T. B. Ottenstein, T. Lompe, M. Kohnen, A. N. Wenz, and S. Jochim, Phys. Rev. Lett. **101**, 203202 (2008).

[5] J. R. Williams, E. L. Hazlett, J. H. Huckans, R. W. Stites, Y. Zhang, and K. M. O'Hara, Phys. Rev. Lett. **103**, 130404 (2009).

[6] G. Barontini, C. Weber, F. Rabatti, J. Catani, G. Thalhammer, M. Inguscio, and F. Minardi, Phys. Rev. Lett. **103**, 043201 (2009).

[7] M. Zaccanti, B. Deissler, C. D'Errico, M. Fattori, M. Jona-Lasinio, S. Müller, G. Roati, M. Inguscio, and G. Modugno, Nat. Phys. **5**, 586 (2009).

[8] N. Gross, Z. Shotan, S. Kokkelmans, and L. Khaykovich, Phys. Rev. Lett. **103**, 163202 (2009).

[9] S. E. Plooack, D. Dries, and R. G. Hulet, Science **326**, 1683 (2009).

[10] M. Berninger, A. Zenesini, B. Huang, W. Harm, H.-C. Nägerl, F. Ferlaino, R. Grimm, P. S. Julienne, and J. M. Hutson, Phys. Rev. Lett. **107**, 120401 (2011).

[11] R. J. Wild, P. Makotyn, J. M. Pino, E. A. Cornell, and D. S. Jin, Phys. Rev. Lett. **108**, 145305 (2012).

[12] S. Knoop, F. Ferlaino, M. Mark, M. Berninger, H. Schöbel, H.-C. Nägerl, and R. Grimm, Nat. Phys. **5**, 227 (2009).

[13] S. Nakajima, M. Horikoshi, T. Mukaiyama, P. Naidon, and M. Ueda, Phys. Rev. Lett. **105**, 023201 (2010).

[14] T. Lompe, T. B. Ottenstein, F. Serwane, K. Viering, A. N. Wenz, G. Zürn, and S. Jochim, Phys. Rev. Lett. **105**, 103201 (2010)

[15] R. S. Bloom, M.-G. Hu, T. D. Cumby, and D. S. Jin, Phys. Rev. Lett. **111**, 105301 (2013).

[16] T. Lompe, T. B. Ottenstein, F. Serwane, A. N. Wenz, G. Zürn, and S. Jochim, Science **330**, 940 (2010).

[17] S. Nakajima, M. Horikoshi, T. Mukaiyama, P. Naidon, and M. Ueda, Phys. Rev. Lett. **106**, 143201 (2011).

[18] B. Huang, L. A. Sidorenkov, R. Grimm, and J. M. Hutson, Phys. Rev. Lett. **112**, 190401 (2014).

[19] S.-K. Tung, K. Jimenez-Garcia, J. Johansen, C. V. Parker, and C. Chin, arXiv: 1402.5943.

[20] R. Pires, J. Ulmanis, S. Häfner, M. Repp, A. Arias, E. D. Kuhnle, and M. Weidemüller, Phys. Rev. Lett. **112**, 250404 (2014).

[21] I. Ferrier-Barbut, M. Delehaye, S. Laurent, A. T. Grier, M. Pierce, B. S. Rem, F. Chevy, and C. Salomon, Science **345**, 1035 (2014).

[22] See Supplemental Material http://link.aps.org/supplemental/10.1103/PhysRevA.90.041603 for the detailed derivation of three-body equations and discussion on the mean-field prediction of $a_{\rm ad}$.

[23] E. Braaten, H.-W. Hammer, D. Kang, and L. Platter, Phys. Rev. A **81**, 013605 (2010).

[24] For the case $x \in (0,1)$, as in the ENS experiment which was mostly carried out in the $a_{\rm bf} < |a_{\rm ff}|$ regime [21], $g(\mathbf{k})$ [Eq. (7)] will have a pole at finite $\mathbf{k}$ and both $f(\mathbf{k})$ and $g(\mathbf{k})$ will become complex. We thus expect that the Bose and Fermi mixtures in the ENS setup will suffer from three-body loss due to the decay of a fermion-fermion dimer to a boson-fermion dimer through three-body collisions.

[25] Here the formulation of $\mathcal{E}$ requires all three scattering lengths to be sufficiently small. It cannot describe the situation when $a_{\rm ad}$ is near resonance, but can give a qualitative picture about how the change of $a_{\rm ad}$ [according to Eq. (1)] affects the stability of the system.

[26] D. S. Petrov, C. Salomon, and G. V. Shlyapnikov, Phys. Rev. Lett. **93**, 090404 (2004).

[27] C. J. Pethick and H. Smith, *Bose-Einstein Condensation in Dilute Gases* (Cambridge University, New York, 2002).

[28] As the first attempt to explore the many-body effect of Eq. (1), here we are only interested in the stability of a homogeneous mixture against density fluctuations. The phase diagram can be further improved by considering the possibility of a separation and collapse of the partially polarized states. These states could exist near the MIX-PS and MIX-CL boundaries, which are not addressed here.

[29] Near the PS-CL phase boundary, $a_{\rm ad}$ goes across a resonance, which is associated with a trimer state emerging from the atom-dimer continuum and the system will suffer an enhanced atom loss near this regime [12–15].

[30] C. Chin, R. Grimm, P. Julienne, and E. Tiesinga, Rev. Mod. Phys. **82**, 1225 (2010).